Long-range oxidation of guanine by Ru(III) in duplex DNA

Michelle R Arkin, Eric DA Stemp*, Sabine Coates Pulver and Jacqueline K Barton

Background: Theoretical and experimental studies have demonstrated that 5′-GG-3′ sequences in DNA are 'hot spots' for oxidative damage, but few studies have definitively addressed whether oxidative damage to DNA may arise from a distance via long-range charge migration. Towards this end, we have prepared tethered ruthenium(Ru)–oligonucleotide duplexes and used a flash–quench strategy to demonstrate long-range charge transport through the DNA double helix.

Results: DNA assemblies containing a tethered Ru(II) intercalator have been synthesized. Ru(III), generated *in situ* in the presence of externally bound electron-transfer quenchers, promotes base damage selectively at the 5′-G of a 5′-GG-3′ doublet located ~37 Å from the binding site of the oxidant. In the absence of a guanine doublet, oxidative damage occurs equally at all guanine bases in the strand. Oxidative damage is also observed at long range for guanine in a G•A mismatch but not in a G•T mismatch.

Conclusions: The present study expands the scope of long-range electron-transfer chemistry in terms of experiments, applications, and possible reactions within the cell. Here we demonstrate oxidative damage to DNA occurring with a high quantum yield over a distance of ~37 Å using a ground-state oxidant. These results point to the equilibration of the radical across the DNA duplex to the sites of lowest energy. In addition, this charge migration is sensitive to the intervening π-stack formed by DNA base pairs and hence may be useful for the detection of mismatches.

Address: Beckman Institute, California Institute of Technology, Pasadena, CA 91125, USA.

*Present address: Mount Saint Mary's College, Los Angeles, CA 90049, USA.

Correspondence: Jacqueline K Barton
E-mail: jkbarton@cco.caltech.edu

Key words: base mismatch, electron transfer, metallointercalator, oxidative DNA repair, radical migration

Received: **19 February 1997**
Revisions requested: **20 March 1997**
Revisions received: **24 April 1997**
Accepted: **28 April 1997**

Chemistry & Biology May 1997, 4:389–400
http://biomednet.com/elecref/1074552100400389

Introduction

It is important to consider radical migration through the DNA double helix in delineating routes to mutagenesis and carcinogenesis [1–3]. Both experiments and theory have explored this issue. For example, radiation biologists have investigated the ionization of DNA by measuring conductivity of DNA [4–6], formation of nucleobase radicals [7–9], and reactivity of intercalated radical traps [10–13] following a pulse of high energy radiation. On the basis of these experiments, researchers have debated whether charge migration can occur over distances ranging from 3 to 200 base pairs (bp) [1]. In another approach, chemists have used spectroscopic tools to monitor photoinduced electron transfer between DNA-bound donors and acceptors ([2,3,14–25]; S.O. Kelley, R.E. Homlin, E.D.A.S. and J.K.B., unpublished results). Results of such studies have suggested that electron transfer reactions are mediated by the π-stacked array formed by the DNA base pairs when the donor and acceptor are intercalated. Theoretical models based on quantum mechanical calculations have also been proposed for the electronic structure of DNA [26–31]. These studies all need to be reconciled in order to understand more fully how radicals affect damage to DNA within the cell.

From a biological perspective, it is essential to determine whether the migration of charge through DNA leads to permanent damage. For this reason, several laboratories have used small molecules as photooxidants to generate ionizing species bound to DNA [29,32–40]. In these studies, damage has been observed primarily at guanine (G), the most easily oxidized base. Furthermore, anthraquinones [34,35,41], napthalimides [29,38], riboflavin [37] and rhodium(III) intercalators [32,33] have been shown to cause oxidative damage selectively at the 5′-G of 5′-GG-3′ sequences; this sequence selectivity has been attributed to preferential binding of the oxidant, perturbations in the DNA sequence, and hole migration through the DNA base stack. Calculations by Saito and coworkers [29] have suggested that sequences containing adjacent guanines show a lowered oxidation potential with the majority of electron density centered on the 5′-G; thus, the extended electronic structure of the DNA base stack may explain the observation that 5′-GG-3′ sequences are 'hot spots' for oxidative damage.

In order to examine directly whether oxidation reactions could occur over long molecular distances, the potent photooxidant and intercalator $Rh(phi)_2(bpy')^{3+}$ [Rh = rhodium; phi = phenanthrenequinone diimine; bpy′ = 4-(carboxybutyl)-4′-methyl-2,2′-bipyridine] was tethered to a DNA oligonucleotide duplex [32]. This assembly provided the first demonstration that DNA oxidation could

Figure 1

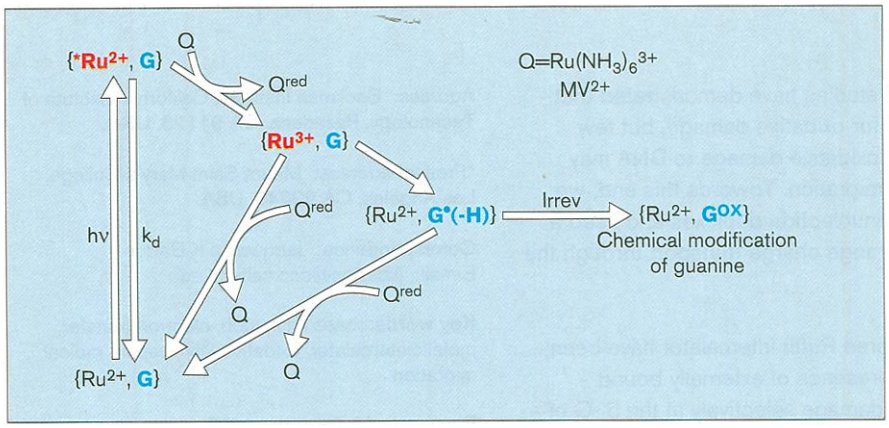

Flash–quench electron transfer cycle. The ground-state intercalating oxidant of DNA, Ru^{3+}, is generated *in situ* by electron transfer to a groove-bound quencher, Q. Once generated, Ru^{3+} promotes oxidation of guanine (G). Recombination reactions with Q^{red} limit the yield, but if Q^{red} is unstable, the yield of damage, G^{ox}, is high.

proceed from a remote position through the DNA π-stack, and damage of 5′-GG-3′ sequences was observed over a distance of ~34 Å. This metallointercalator was also shown to cause the catalytic repair of thymine dimers in duplex DNA over distances of 17–26 Å [42]. Work with tethered Rh(III) photooxidants thus indicates that the DNA π-stack can mediate chemistry at a distance.

We recently reported the application of a flash–quench methodology for oxidizing guanine within the DNA duplex using $Ru(phen)_2dppz^{2+}$ [Ru = ruthenium; phen = 1,10-phenanthroline; dppz = dipyridophenazine] (Figure 1; [43]). Complexes of Ru(II) bearing dipyridophenazine ligands have been extensively studied as luminescent probes of DNA due to the large (~10^3) enhancements in emission observed upon DNA intercalation [14,44–47]. A flash–quench cycle using polypyridyl complexes of Ru(II) has been devised by Gray and coworkers [48] for the spectroscopic study of protein-mediated electron transfer; moreover, the well-characterized spectroscopy of Ru(II) complexes can be exploited in the study of electron transfer chemistry between Ru(II) intercalators and DNA [49].

As shown in Figure 1, the flash–quench reactions are initiated by visible light which generates an excited Ru(II) complex, *Ru(II). Intercalated *Ru(II) is then quenched by a nonintercalating electron acceptor Q to form Ru(III); this species can be reduced back to Ru(II) either through bimolecular recombination with reduced quencher Q^{red} or by electron transfer with a nearby guanine base. Spectroscopy studies are consistent with the formation of the neutral guanine radical, G•(–H), resulting from deprotonation of a guanine cation radical. The oxidized guanine radical can then return to its resting state by reaction with the reduced quencher or undergo further reaction with O_2 or H_2O to form the stable oxidation product(s) G^{ox}. Using transient absorption spectroscopy, we have monitored the formation and decay of the guanine radical formed by the flash–quench cycle in poly(dG–dC) and in a mixed sequence of DNA [43].

It is noteworthy that the method described in Figure 1 is not purely a reaction cycle, but rather a method for generating stable products. Kochevar and coworkers [36] have performed an analogous experiment in DNA with ethidium as an intercalated donor and methyl viologen (MV^{2+}) as a quencher; using gel electrophoresis, these authors demonstrated single-strand breaks at all guanine bases. We find that the flash–quench methodology yields permanent damage at 5′-GG-3′ and 5′-GGG-3′ sequences following continuous irradiation. The quantum yield of oxidative damage (Φ_{damage}) was found to be modulated by the choice of quencher; unstable Q^{red} leads to greater amounts of G^{ox}. The ability to tune the yield of oxidative damage readily is an important advantage of the flash–quench method over photooxidation.

Here, we use a flash–quench experiment to demonstrate oxidation of 5′-GG-3′ sequences by intercalated Ru(III) when the reactants are separated by 11 bp (37 Å) of duplex DNA. To prepare a system in which the separation between Ru(III) acceptor and DNA donor is well defined, we have tethered $Ru(phen)(bpy')(Me_2dppz)^{2+}$ [Me_2dppz = 9,10-dimethyl-dipyridophenazine] to an oligonucleotide duplex to produce Ru(II)–DNA. The site of Ru(II) intercalation is determined by $^1O_2$-sensitized damage of nearby guanine bases, thus providing an approximation of the distance between the Ru(III) oxidant and 5′-GG-3′. Additionally, we explicitly compare oxidative damage in an oligonucleotide duplex containing 5′-GC-3′ in place of a 5′-GG-3′ sequence and also explore the effects of base mismatches on the oxidation of guanine both within and beyond the mismatch. Taken together, these results demonstrate, in a well-defined chemical experiment, that long-range charge migration can occur in DNA. These experiments expand the scope of DNA-mediated electron

Figure 2

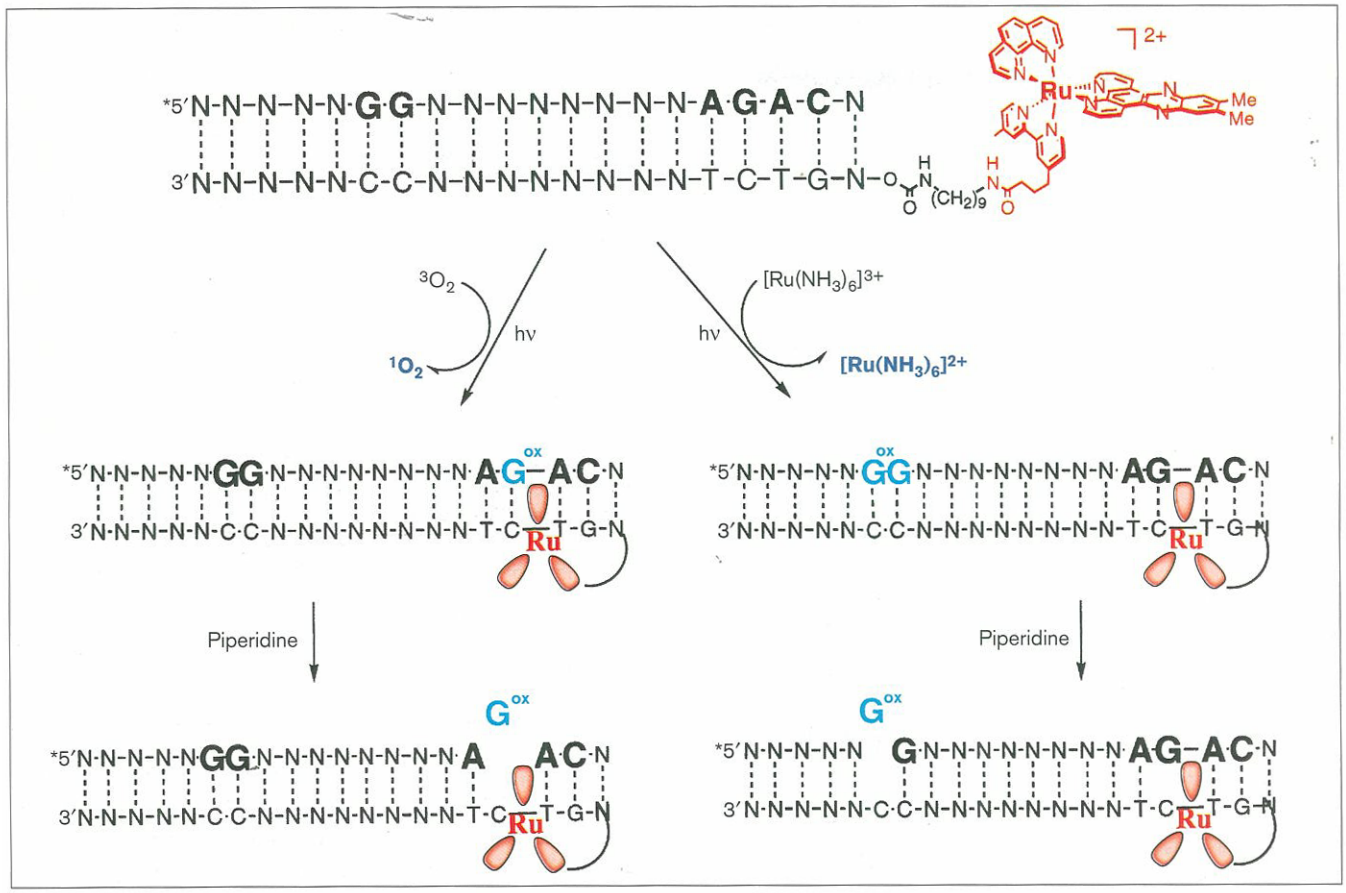

Schematic illustration of oxidation reactions. The position of binding can be monitored by $^1O_2$ sensitization (left pathway). The $^1O_2$, sensitized by *Ru(II), reacts with nearby guanine bases; oxidation products are revealed as strand breaks after treatment with piperidine. Long-range electron transfer from guanine is initiated by excitation of Ru(II) in the presence of externally bound, oxidative quenchers such as $Ru(NH_3)_6^{3+}$ or MV^{2+} (right pathway). Electron transfer from *Ru(II) to the quencher creates a hole on the Ru(III) intercalator; this hole is filled by back-reaction with reduced quencher or by oxidation of guanine. Piperidine treatment reveals the ultimate site of guanine base oxidation.

transfer reactions by using a ground-state oxidant to produce long-range oxidative damage in high yield over a well-defined distance.

Results and discussion

Intercalation of Ru(II)–DNA conjugates

Figure 2 illustrates how we determine the sites of Ru(II) intercalation and base oxidation. Intercalation by the pendant Ru(II) complex is measured by singlet oxygen ($^1O_2$) sensitization (left pathway), because irradiation of Ru(II) polypyridyl complexes in the presence of DNA and O_2 leads to $^1O_2$ damage at guanine residues [50,51]. For the first time, we use this technique to establish the site of intercalation of a dppz complex of Ru(II). In contrast to $^1O_2$-sensitization, the flash–quench experiment (right pathway) uses the ground state Ru(III), formed by quenching of *Ru(II) by externally bound Q, to oxidize DNA at the site of lowest oxidation potential. The resultant base damage is revealed by strand scission following treatment with hot piperidine [52]. Moreover, since only the dppz ligand is intercalated into DNA, a significant portion of the octahedral Ru(II) complex is accessible to solvated reactants such as O_2. Hence, by photolyzing the oligonucleotide assemblies in the absence and presence of electron transfer quenchers, we can assay both the position of intercalation and the yield of base oxidation.

Figure 3 presents the damage caused by the $^1O_2$ and flash–quench experiments on an oligonucleotide containing tethered Δ-Ru(phen)(bpy′)$(Me_2dppz)^{2+}$ and one 5′-GG-3′ doublet. The oligonucleotide 5′-TGATC*GG*TGCGTCT-GAGACT-3′ was 5′-^{32}P-end-labeled and hybridized to the 5′-ruthenated complement, as shown in Figure 3b. Lane 2 (Figure 3a) shows $^1O_2$-sensitized damage generated by irradiation of Ru(II)–DNA (8 μM) with visible light followed by hot piperidine treatment. Cleavage occurs primarily at the guanine closest to the site of Ru(II) attachment indicating that the complex is bound only in that region of the

Figure 3

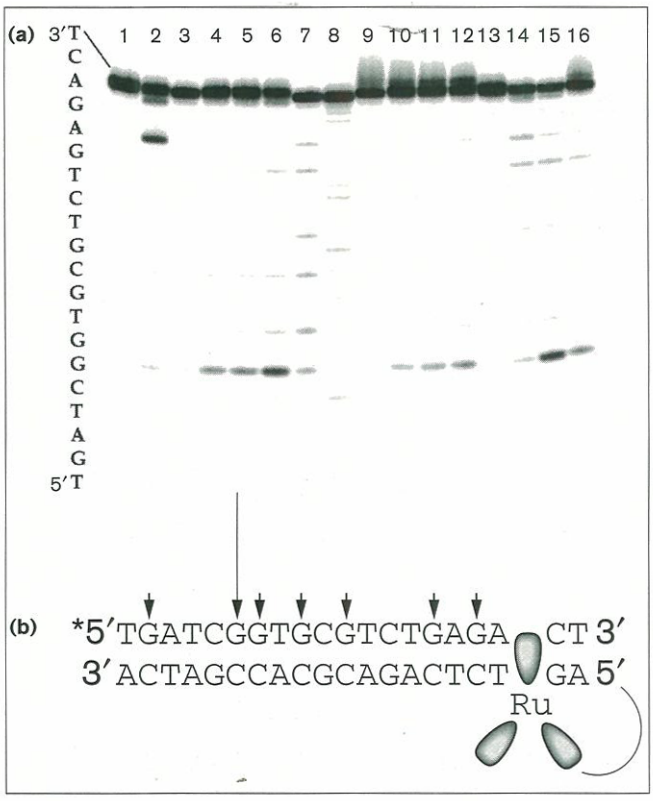

(a) Autoradiogram after 20% denaturing polyacrylamide gel electrophoresis showing oxidation reactions of Ru(II)–DNA. The oligonucleotide 5′-TGATCGGTGCGTCTGAGACT-3′ was 5′-^{32}P-end-labeled, hybridized to Ru(II)-labeled complement or to unmodified strand, and irradiated as described in the Material and methods section. Samples shown are as follows: lanes 1 and 13, Ru(II)–DNA without irradiation; lane 2, Ru(II)–DNA irradiated for 60 min in the absence of quencher; lane 3, unmetallated DNA + MV^{2+} irradiated for 5 min; lanes 4–6, Ru(II)–DNA + MV^{2+} irradiated for 1, 2, 5 min, respectively; lanes 7 and 8, Maxam–Gilbert sequencing reactions G and C+T, respectively; lane 9, unmetallated DNA with $Ru(NH_3)_6^{3+}$ irradiated for 30 min; lanes 10–12, Ru(II)–DNA + $Ru(NH_3)_6^{3+}$ irradiated for 10, 20, 30 min, respectively; lane 14, $Ru(phen)_2(dppz)^{2+}$ + DNA, irradiated for 60 min; lane 15, $Ru(phen)_2(dppz)^{2+}$ + DNA with MV^{2+} irradiated for 5 min; lane 16, $Ru(phen)_2(dppz)^{2+}$ + DNA with $Ru(NH_3)_6^{3+}$ irradiated for 30 min. Lamp power in these experiments was ~6 mW at 442 nm. **(b)** Oxidative damage of the oligonucleotide duplex by Δ-Ru(phen)(bpy′)$(Me_2dppz)^{3+}$-DNA. Arrow heights reflect the relative cleavage intensity. The position of intercalation is estimated on the basis of $^1O_2$ sensitization.

Figure 4

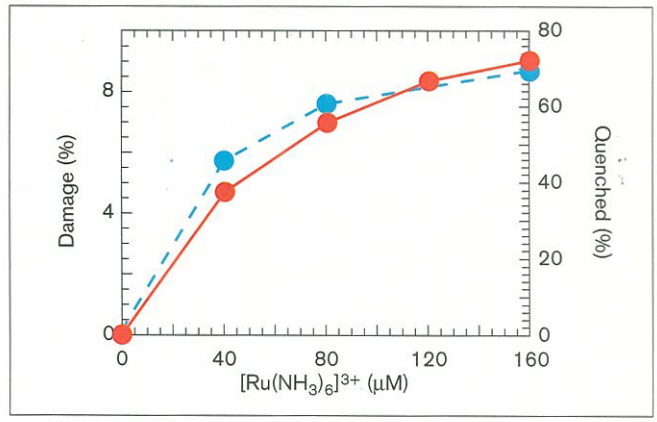

Plot showing the yield of piperidine-labile DNA damage (blue circles) and the fraction of emission quenching of tethered Δ-Ru(phen)(bpy′)$(Me_2dppz)^{2+}$ (red circles) as a function of concentration of $Ru(NH_3)_6^{3+}$. Samples contained 5′-TGATCGGTGCGTCTGAGACT-3′ hybridized to Ru(II)-modified complement (8 μM duplex) in a buffer of 5 mM phosphate, 50 mM NaCl, pH 7. The fraction of oxidative damage was determined by phosphorimagery of ^{32}P-labeled DNA; the fraction of emission quenching was measured by integration of time-resolved luminescence decays at 616 nm.

oligonucleotide duplex. Previous studies have indicated that the rate constant for the oxidation of guanine by $^1O_2$ is ~100-fold greater than for the reaction with the other nucleobases [53]. Therefore, only damage at guanine is expected under these experimental conditions. Intercalation of this metal complex is supported by the strong emission of Ru(II)–DNA, by hypochromicity in the Me_2dppz absorption band, and by a 3°C increase in melting temperature of Ru(II)–DNA compared to the unmetallated 20 bp duplex (data not shown). As expected, the extent of $^1O_2$-sensitized damage also increases twofold for Ru(II)–DNA in D_2O compared to H_2O (45% compared to 20% cleavage after 1 h irradiation), because D_2O increases the lifetimes of both $^1O_2$ and *Ru(II) [54,55]. These data demonstrate that $^1O_2$ sensitization can be used to mark the site of intercalation.

In contrast to the specific $^1O_2$-sensitized damage observed for Ru(II)–DNA, all guanine residues are damaged when $Ru(phen)_2dppz^{2+}$ is noncovalently bound to the oligonucleotide duplex (Figure 3a; lane 14). The lower cleavage intensity observed in lane 14 compared to lane 2 is likely to be due to the fourfold lower emission quantum yield ($\Phi_{emission}$) of $Ru(phen)_2dppz^{2+}$ compared to Δ-Ru(phen)(bpy′)$(Me_2dppz)^{2+}$ (0.007 compared to 0.03, respectively) and due to the specific binding of the tethered complex.

Long-range oxidative damage

In the flash–quench experiment, we add an electron transfer quencher, photolyze Ru(II)–DNA, and monitor the yield and position of damage to DNA initiated by electron transfer. As predicted by experiments with noncovalently bound $Ru(phen)_2dppz^{2+}$ [43], oxidative damage to DNA is observed at the 5′-G of the 5′-GG-3′ doublet. Importantly, this 5′-GG-3′ doublet is placed 11 bp away from the Ru binding site, and thus damage is observed ~37 Å from the Ru(III) reactant. As shown in Figure 3, this reaction requires light (lane 1), quencher (lane 2), Ru(phen)(bpy′)$(Me_2dppz)^{2+}$ (lanes 3,9), and piperidine treatment (not shown).

Table 1

Parameters for flash-quench cycle with Δ-Ru(phen)(bpy')(Me_2dppz)-DNA*.

Quencher	equivalents Q	% quenching†	k_q ‡	Φ_{damage} §
$[Ru(NH_3)_6]^{3+}$	20	73	$4.1 \times 10^{10}\ M^{-1}s^{-1}$	1.3×10^{-5}
methyl viologen^{2+}	10	13	$5.2 \times 10^{9}\ M^{-1}s^{-1}$	2×10^{-3}

*Conditions are: 8 μM Ru(II)–5′-AGTCTCAGACGCACCGATCA-3′ hybridized to complement in an aerated buffer of 5 mM phosphate, 50 mM NaCl, pH 7. †Measured by steady-state emission; uncertainty is ~5%. ‡$I_o/I = 1 + [Q](k_q/k_{obs})$; k_{obs} = weighted average of a biexponential fit of *Ru(II) emission, $k_1 = 1.8 \times 10^6\ s^{-1}$ (60%), $k_2 = 3.4 \times 10^6\ s^{-1}$ (20%), k_q = quenching rate constant. Uncertainty is ~10%. §Φ_{damage} = ratio of the yield of piperidine-mediated strand breaks at the 5′-G of 5′-GG-3′ doublets to Φ_{ET}. $\Phi_{ET} = \tau\ k_q[Q]$, where τ is the average emission lifetime in the presence of Q. Uncertainty in Φ_{damage} is ~20%.

As in experiments with noncovalently bound Ru(II) intercalators [43], the yield of the guanine oxidation reaction in Ru(II)–DNA is modulated by the choice of quencher. For the quenchers methyl viologen (MV^{2+}) and $Ru(NH_3)_6^{3+}$, damage increases with irradiation time (Figure 3; lanes 4–6, lanes 10–12, respectively) and with the concentration of quencher (Figure 4). Damage also correlates with the instability of the reduced quencher; as described in Table 1, the yield of damage in the presence of MV^{2+} is ~100-fold higher than with $Ru(NH_3)_6^{3+}$. $Ru(NH_3)_6^{2+}$ formed in the quenching reaction can efficiently re-reduce both intercalated Ru(phen)(bpy')(Me_2dppz)$^{3+}$ and G•(–H). By contrast, MV^+ is known to react readily with dissolved O_2 to form MV^{2+} and superoxide, with a rate constant of $\sim 10^9\ M^{-1}s^{-1}$ [56]. We have obtained evidence for this reaction by transient absorption spectroscopy; the rapidly formed MV^+ is found to decay on the 100 μs timescale (λ_{obs} = 380 nm), whereas Ru(III) decays on a longer timescale [43]. The rapid loss of MV^+ thus permits increased formation of G•(–H) by electron transfer with long-lived Ru(III). Superoxide has previously been shown to react with G•(–H), thereby providing a pathway for reformation of guanine [34]. Thus the yield of irreversible damage is greater when Ru(III) and G•(–H) cannot be readily reduced by Q^{red}. Moreover, because the damage yield depends sensitively upon the character of the quencher, the oxidation cannot be a result of any excitation of guanine.

Table 1 lists the quantum yield of damage (Φ_{damage}) to the 5′-G of 5′-GG-3′ doublets. Note that only *Ru(II) complexes which are oxidatively quenched provide the oxidizing species Ru(III); for example only 13% of *Ru(II) react with 10 equivalents of MV^{2+} giving a damage yield of 0.002. As shown in Figure 4, the yield of Ru(III) formed and the guanine oxidation observed increase concomitantly with quencher. The flash–quench method therefore allows the yield of guanine oxidation to be modulated in two ways: by changing the efficiency of Ru(III) formation or by changing the rate of recombination of Ru(III) or G•(–H) with Q^{red}.

In order to characterize the product of guanine oxidation, Ru(II)–DNA was irradiated in the presence of $Ru(NH_3)_6^{3+}$ and then subjected to enzymatic digestion [37]. Quenching by $Ru(NH_3)_6^{3+}$ leads to significant production of 8-oxo-G products as identified by high performance liquid chromatography (HPLC; Figure 5); analysis of the products formed by MV^{2+}-induced oxidation was complicated by the coelution of methyl viologen and the nucleosides dG, dT, and d8-oxo-G. We sought to correlate the yield of strand scission with the yield of 8-oxo-G obtained in the presence of $Ru(NH_3)_6^{3+}$, and found that 8-oxo-G was the major product [32,34,37,57]. Although it is difficult to quantitate the total amount of strand scission because there are several guanine residues on the unlabeled DNA strand, we estimate that the yields of piperidine-labile sites and 8-oxo-G are the same within a factor of two. Thus, the flash–quench

Figure 5

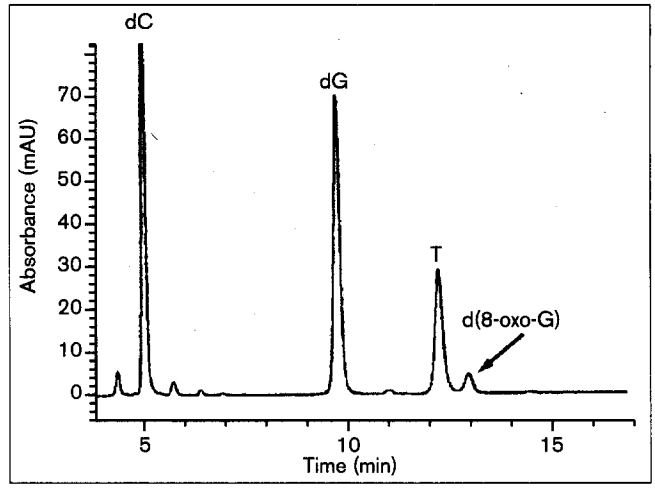

HPLC traces of nucleosides produced by enzymatic digestion of damaged oligonucleotides. The duplex 5′-TGATCGGTG-CGTCTGAGACT-3′ hybridized to Ru(phen)(bpy')(Me_2dppz)$^{2+}$-modified complement (10 μM) was irradiated in the presence of $Ru(NH_3)_6^{3+}$ (200 μM). The oligonucleotide was then subjected to digestion with nuclease P_1 and alkaline phosphatase and analyzed by HPLC chromatography (λ_{obs} = 295 nm). The retention time for 8-oxo-G was 9.2 min. The product was identified by UV–visible absorption and coelution with authentic standard.

Figure 6

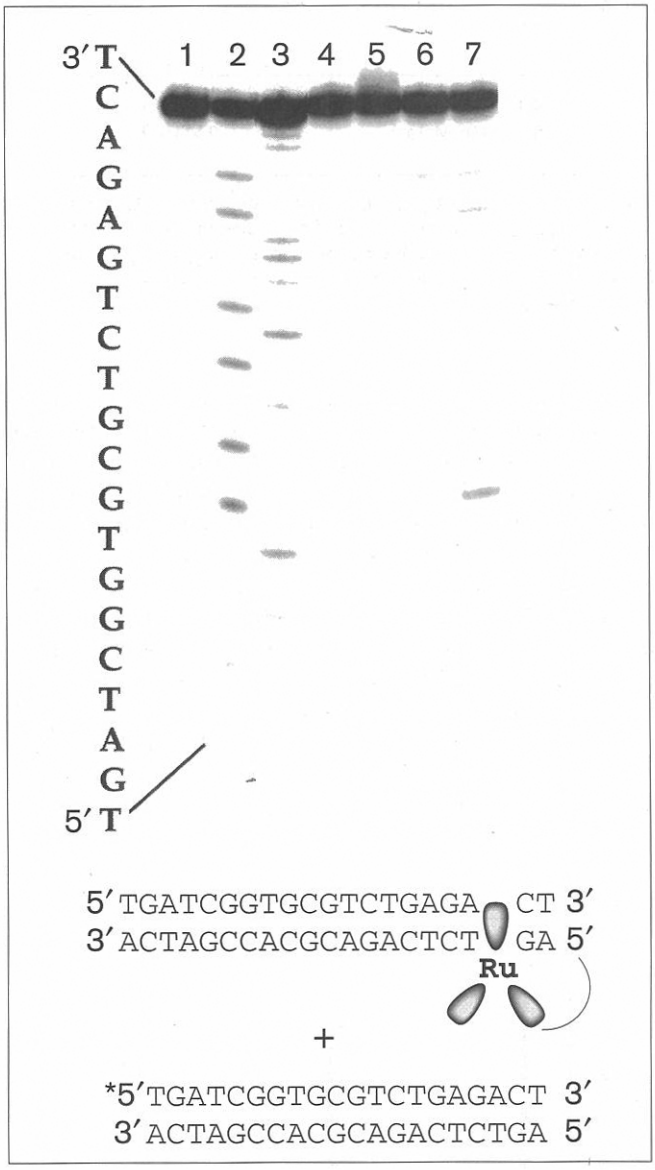

Autoradiogram after 20% denaturing polyacrylamide gel electrophoresis monitoring the extent of interduplex 5′-GG-3′ oxidation. 5′-^{32}P-TGATCGGTGCGTCTGAGACT-3′ was hybridized to unmetallated complement and incubated with unlabeled Ru(II)–DNA of the same sequence. Samples shown are as follows: lane 1, ^{32}P-DNA without irradiation; lanes 2 and 3, Maxam–Gilbert sequencing reactions G and C+T, respectively; lane 4, Ru(II)–DNA + ^{32}P-DNA irradiated for 60 min; lane 5, Ru(II)–DNA + ^{32}P-DNA + $Ru(NH_3)_6^{3+}$ irradiated for 30 min; lanes 6 and 7, Ru(II)–DNA + ^{32}P-DNA + MV^{2+} irradiated for 1 min and 5 min, respectively.

oxidation reaction yields the primary oxidative DNA lesion found within the cell [58,59].

Diffusion versus long-range oxidation

We can distinguish long-range oxidation in the flash–quench experiment from a reaction mediated by a diffusible species. First, the $^1O_2$ pattern (Figure 3, lane 2) exemplifies damage caused by a reactive, diffusible species generated at the Ru(II) binding site; damage is strongest nearest the Ru(II) and tapers off as the distance from the site increases. It is noteworthy that the yield of $^1O_2$-sensitized damage is minimal under conditions where long-range oxidative damage is observed. Additionally, we monitored the oxidative damage of a radiolabeled DNA duplex in the presence of unlabeled Ru(II)–DNA (Figure 6) and found that no damage occurs to the radiolabeled but unmetallated duplex when the quencher is $Ru(NH_3)_6^{3+}$ (lane 5). This control experiment indicates that $Ru(NH_3)_6^{2+}$ does not damage DNA, that Δ-Ru(phen)(bpy′)$(Me_2dppz)^{3+}$ is only intercalated into the DNA helix to which it is covalently attached, and that damage is not caused by a species which can diffuse to another duplex. Using $Ru(NH_3)_6^{3+}$ as quencher, we detect no intermolecular damage at high phosphorimager sensitivity. When this experiment is repeated using MV^{2+} as quencher, no interstrand damage is observed after 1 min of irradiation (lane 6) and minimal damage (~10% of intramolecular damage) at 5′-GG-3′ is observed after 5 min of irradiation. We attribute this cross-reactivity to a small amount of long-lived Ru(III) intercalating into other duplexes, because the decay of Δ-Ru(phen)(bpy′)$(Me_2dppz)^{3+}$ ($k \sim 10^2$ s^{-1}) [43] occurs on a timescale that is similar to the dissociation of this intercalator ($k \sim 10^3$ s^{-1}) [47]. Similar results for both quenchers were obtained when the labeled duplex was identical to the metallated DNA (Figure 6) or when the ^{32}P-labeled duplex had a different sequence from Ru(II)–DNA; thus, the rates of strand exchange are negligible in these experiments. Taken together, these data indicate that oxidation of 5′-GG-3′ by Ru(III) is affected by complexes intercalated into DNA, not by a diffusible species, and thus occurs between reactants separated by ~11 bp.

Oxidation of DNA containing no 5′-GG-3′ sequences

We have also considered long-range oxidation in an oligonucleotide duplex constructed without a 5′-GG-3′ doublet (Figure 7), using a sequence which differs by only one base pair from the duplex shown in Figure 3. These experiments form a bridge between spectroscopic studies which indicate that guanine radicals are formed when poly(dG-dC) is oxidized by Ru(III) and gel electrophoresis experiments which indicate that permanent damage occurs primarily at 5′-GG-3′ doublets [43]. When no 5′-GG-3′ sequences are present, oxidative damage is observed at all guanine residues on the labeled strand, with no large sequence preference or sensitivity to the distance from the oxidant (Figure 8). The total reaction on the duplex is comparable to that seen with the duplex containing 5′-GG-3′ in Figure 3. Such comparisons can only be made qualitatively, given the different reaction conditions; however, it is important that the cleavage observed in Figure 7 is not simply the background damage observed at other guanine residues in Figure 3. These results suggest that radical

Figure 7

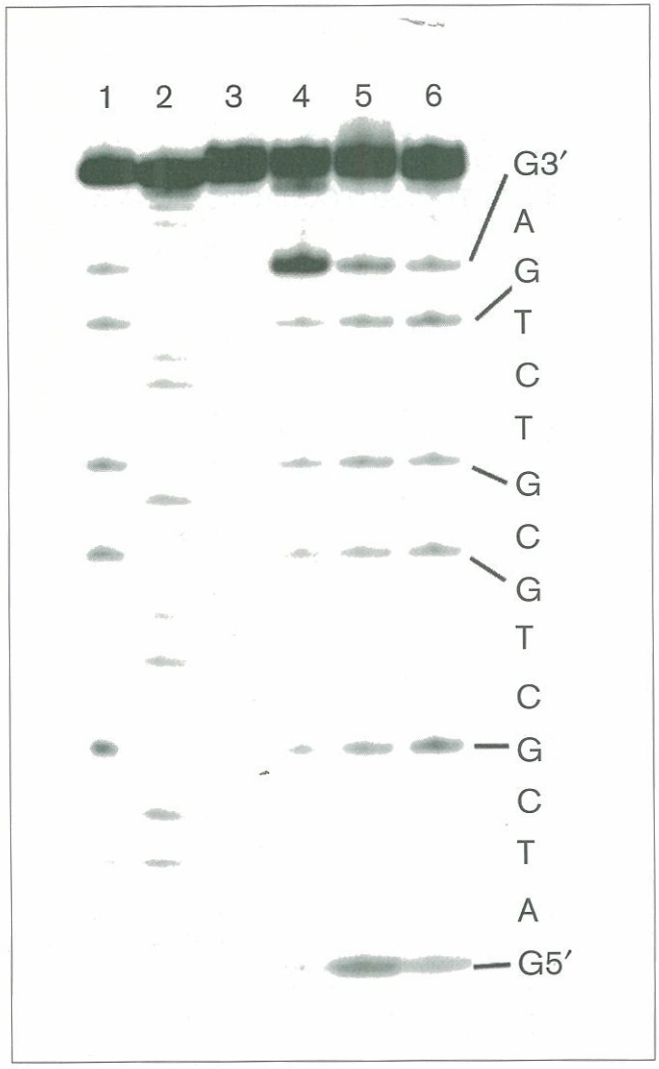

Autoradiogram after 20% denaturing polyacrylamide gel electrophoresis showing oxidation reactions of Ru(II)–DNA. The oligonucleotide 5′-TGATC*GC*TGCGTCTGAGACT-3′ was 5′-^{32}P-end-labeled, hybridized to Ru(II)-labeled complement and irradiated as described in the Materials and methods section. Samples shown are as follows: lanes 1 and 2, Maxam–Gilbert sequencing reactions G and C+T, respectively; lane 3, unirradiated Ru(II)–DNA; lane 4, Ru(II)–DNA irradiated for 60 min; lane 5, Ru(II)–DNA + $Ru(NH_3)_6^{3+}$ irradiated for 30 min; lane 6, Ru(II)–DNA + MV^{2+} irradiated for 5 min.

damage is able to migrate to the site of lowest redox potential, where a fraction of the radical is subsequently trapped to yield permanent damage [29,34]. In the absence of a low energy site, the radicals become evenly distributed over the 20 bp DNA duplex on a timescale which is faster than that of trapping. The striking difference in the pattern of oxidation evident with only a single base change argues against any transient openings in the intervening DNA structure in accounting for long-range oxidation. These results are also consistent with Rh(III) photooxidation systems, in which

Figure 8

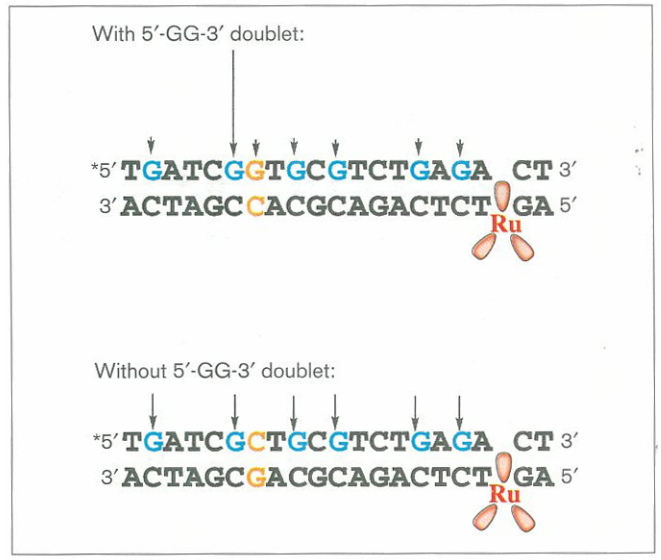

Oxidative damage caused by tethered Δ-Ru(phen)(bpy′)$(Me_2dppz)^{3+}$ in the oligonucleotide duplex containing a 5′-GG-3′ doublet (Figure 3) and in the mutated duplex containing a 5′-GC-3′ sequence (Figure 7). Arrow heights reflect relative cleavage intensity. The position of intercalation is estimated based on $^1O_2$ sensitization.

two 5′-GG-3′ sequences placed in the same oligonucleotide were damaged with similar efficiencies [32]. These observations graphically underscore the notion of an equilibration of a radical across the DNA duplex.

Mismatches

We have also investigated the effects of a single base mismatch on the long-range oxidation of guanine both within and beyond the mismatch. Figure 9 presents the damage caused by the $^1O_2$ experiment on oligonucleotides containing tethered Ru(phen)(bpy′)$(Me_2dppz)^{2+}$, a G•A or G•T mispair placed ~5 bp, and a single 5′-GG-3′ sequence placed ~11 bp from the Ru(II) binding site. In these experiments, the oligonucleotide sequence 5′-ACGAC*GG*-TGAC*GC*TGAGACT-3′ was 5′-^{32}P-end-labeled and hybridized to 5′-ruthenated complement. Lanes 2, 6, and 10 show $^1O_2$-sensitized damage in the assemblies containing the fully complementary sequence, the G•A mismatch, and the G•T mismatch, respectively. As anticipated, cleavage is observed only at the guanine that is closest to the site of Ru(II) attachment, indicating that the complex is intercalated into the oligonucleotide duplex.

Also shown in Figure 9 are the results of the flash–quench experiment on these Ru–DNA duplexes utilizing MV^{2+} as the external quencher. In the fully complementary assembly, guanine damage is evident only at the 5′-GG-3′ doublet (lanes 3–5). In contrast, duplex containing a G•A mismatch displays oxidative damage both at guanine of the mispair and at the more distal 5′-GG-3′ doublet (lanes 7–9).

Figure 9

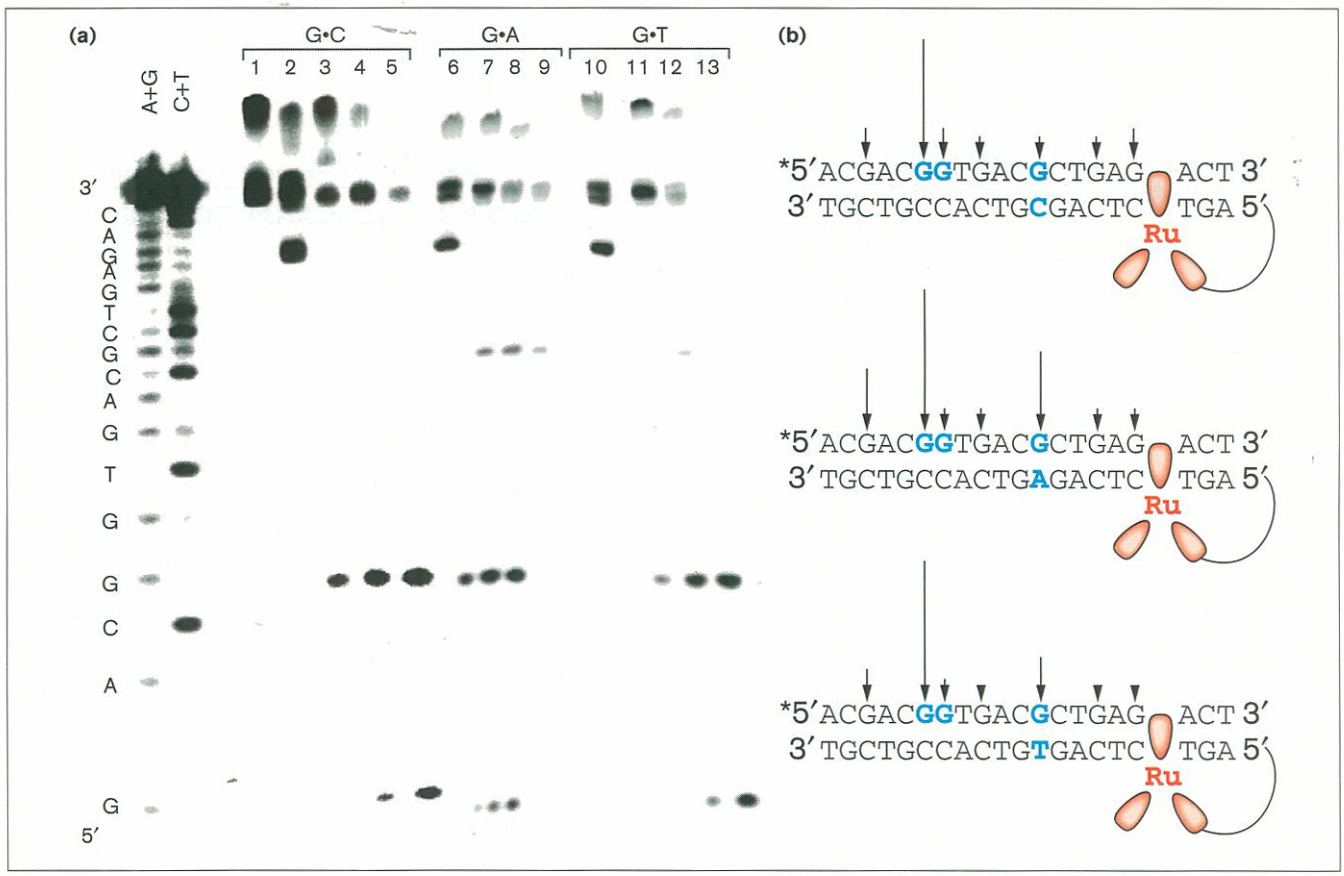

Comparison of long-range oxidative damage on Ru(II)-modified DNA in a complementary duplex and in duplexes containing a G•A or G•T mismatch. **(a)** Autoradiogram after 20% denaturing polyacrylamide gel electrophoresis monitoring the extent of G oxidation by Ru–DNA. The oligonucleotide 5′-ACGAC*GG*TGAC*G*CTGAGACT-3′ was 5′-^{32}P-end-labeled, hybridized to Δ-Ru(II)-modified complement, irradiated and piperidine treated as described in the Materials and methods section. It should be noted that for the fully complementary assembly the Δ-enantiomer of the Ru(II)–DNA conjugate could not be isolated, so experiments were conducted using *rac*-Ru(II)–DNA. The lanes labeled A+G and C+T correspond to Maxam–Gilbert sequencing reactions. Lanes 1–5 present data from studies of complementary duplex (G•C): lane 1, Ru–DNA without irradiation; lane 2, Ru–DNA irradiated for 60 min in the absence of quencher; lanes 3–5, Ru–DNA + MV^{2+} irradiated for 1, 2, 5 min, respectively. Lanes 6–9 present data from duplex containing a G•A mismatch (G•A): lane 6, Ru–DNA irradiated for 60 min in the absence of quencher; lanes 7–9, Ru–DNA + MV^{2+} irradiated for 1, 2, 5 min, respectively. Lanes 10–13 present data from duplex containing a G•T mismatch (G•T): lane 10, Ru–DNA irradiated for 60 min in the absence of quencher; lanes 11–13, Ru–DNA + MV^{2+} irradiated for 1, 2, 5 min, respectively. It should be noted that the guanine damage seen at the base of the gel is artificially high; the parent bands indicate that the DNA has been overcleaved for Ru–DNA + MV^{2+} irradiated for 2 min and 5 min. This is likely to be a function of high lamp power (~70 mW at 442 nm) during the experiment. **(b)** Oxidative damage of G•C, G•A and G•T oligonucleotide duplexes by Ru(phen)(bpy′)$(Me_2dppz)^{3+}$–DNA. Arrow heights reflect relative cleavage intensity. The position of intercalation is estimated based on $^1O_2$ sensitization.

The results of the flash–quench experiment are notably different when the more destabilizing G•T mismatch is substituted at the G•X site. Lanes 11–13 reveal that although the 5′-GG-3′ doublet is oxidized, only minimal damage of guanine at the mismatch site is observed. Thus, the flash–quench methodology provides a sensitive probe for detecting a G•A mismatch within duplex DNA.

These observations suggest that guanine oxidation at a mismatch is a function of increased solvent accessibility of the G•A over G•T mismatch and/or differing redox potentials of guanine residues. These two possibilities are predicted to affect the rates of different steps in the flash–quench experiment; solvent accessibility would modulate the rate of reaction between G•(–H) and O_2 or H_2O to generate G^{ox}, while oxidation potential would affect the formation of G•(–H). While there are no direct studies of the variation of redox potential with base mismatches, there have been several studies addressing the differences in structure between the G•A and G•T mismatch [39,60–62]. These have shown that distortions are highly localized to the base pair site, that the G•A mismatch is most structurally similar

to a Watson–Crick base pair, and that the two H-bonds in the G•T mismatch direct the thymine into the major groove and the guanine towards the minor groove relative to Watson–Crick base pairs. Interestingly, X-ray crystallography of an oligonucleotide duplex containing a G•T mispair shows a highly ordered network of solvent molecules surrounding the base mismatch [61]. The reactivities of these two mismatches have also been probed by cyclic voltammetry [39]. Using the nonintercalating $Ru(bpy)_3^{3+}$, Thorp and coworkers [39] found that G•A mismatches were more readily oxidized than G•T base pairs; the difference in oxidation rates in this case was attributed to the accessibility of guanine in the minor groove. It is noteworthy that, in contrast to our studies using a remotely-placed intercalator, the geometry of electron transfer reactions between $Ru(bpy)_3^{3+}$ and DNA are 'perpendicular' to the DNA base stack. Thus Ru(III) oxidants are able to differentiate mismatches both from within the DNA base stack and by diffusion to the DNA groove.

As discussed above, one consequence of a mismatch in duplex DNA is a localized disruption of the helix. We also may investigate the effect of such a distortion on guanine oxidation by comparing the relative amount of damage observed at the 5′-GG-3′ doublet in duplexes containing either a G•A or a G•T mismatch. It should be noted that in this comparison the fully complementary assembly is not included because only the racemate of this particular Ru(II)–DNA conjugate could be isolated, and previous work has demonstrated a difference in DNA electron transfer reactions between Λ and Δ isomers [14,32]. For the assemblies containing a mismatch, $^1O_2$-sensitization reveals equal damage at the Ru(II) intercalation site, suggesting that the complex is well intercalated in both sequences. In the Ru(II)–DNA oligonucleotide duplex containing the G•A mismatch, 16% guanine damage is observed at the distal 5′-GG-3′ doublet, but only 10% damage is observed at that site in the presence of the more disruptive G•T mispair. A similar sensitivity to helix disruption has been observed for photooxidation of a GG doublet distal to a DNA base bulge [33]. Both results indicate that long-range guanine oxidation is sensitive to the intervening DNA base stacking.

Comparison of flash–quench and photooxidation with metallointercalators

It is valuable to compare Ru(III) oxidation of guanine residues with reactions caused by photooxidants [32,34,37,38]. In some respects, the characteristics of long-range oxidation should be identical in both systems, since they seem to differ only in the method of hole generation on the intercalator. Some similarities have been observed, for example, between $Ru(phen)(bpy')(Me_2dppz)^{3+}$ and $*Rh(phi)_2(bpy')^{3+}$ (*Rh(III)) [32]. Both experiments use tightly bound metallointercalators, and we have shown that both reactions can occur over distances of ~30 Å with the same sequence-selectivity of damage and the same final product, 8-oxo-G.

There are, however, important differences between the Ru(III) and *Rh(III) systems. Possible advantages of the flash–quench system include high damage yields, long wavelength of irradiation, and tunability of the oxidation potential of the Ru(II) donor. First, the quantum yields for oxidative damage are ~10^3–10^5-fold higher for the flash–quench system than for the *Rh(III) systems, and suitable quenchers can be chosen for a particular experiment. For example, the good stability and low absorptivity of $Ru(NH_3)_6^{3+}$ make it ideal for photophysical measurements, while MV^{2+} gives high yields and thus permits short irradiation times. Second, in contrast to the $Rh(phi)_2(bpy')^{3+}$ photooxidant which shows evidence of direct photocleavage of DNA at 365 nm [32,63], the flash–quench reactions result in a very low background of DNA damage. This relatively clean reaction results from the long wavelength of irradiation and high photochemical stability of Ru(II) polypyridyl complexes. Finally, we expect that the reactivity and sequence-selectivity of oxidation reactions may be tuned by varying the redox potential of the Ru(II) complex. In this context, the use of tris(heteroleptic) complexes greatly increases the number of tethered Ru(II) intercalators that may be synthesized [64].

The photooxidation systems provide other advantages [32,34,37,38]. The flash–quench cycle, as described, uses diffusible species which can complicate the experiment, particularly if other noncovalent interactions, such as protein–DNA binding, are involved. Additionally, Rh(III) photooxidation systems allow a more detailed analysis of the intercalation site, because phi complexes of Rh(III) are known to photocleave the backbone of DNA directly at the site of binding [32,63]. The contrasts between these two experimental systems should direct the choice of oxidant in future studies.

Perhaps the most important point is that both *Rh(III) and ground-state Ru(III) intercalators can affect the same guanine oxidation chemistry. Contrasting the energetics and timescales of these two systems could therefore provide insight into the reaction mechanism(s). For example, because the reactive forms of the two metal complexes are likely to have different energies, it appears that the long-range oxidation of DNA is not highly sensitive to the energy of the generated hole. Additionally, the difference in Φ_{damage} observed for these two systems could relate to the timescales for the two reactions; the *Rh(III) lifetime is less than 100 ns [65], whereas Ru(III) is stable for hundreds of microseconds [43]. The difference in yields is unlikely to be due to the thermodynamic driving force, because *Rh(III) has a reduction potential of 2V [65], whereas Ru(III) has a reduction potential of 1.6V [14]. Further comparisons between photooxidation and

ground-state hole formation will help define the parameters for long-range oxidative damage of DNA.

Significance

Mobile positive and negative charges, generated in duplex DNA by ionizing radiation, have been suggested to be a significant source of the DNA damage that causes mutagenesis and, eventually, cancer. Researchers have also used DNA-binding molecules as photooxidants to cause oxidative damage in DNA. These studies have shown that 5′-GG-3′ sequences are 'hot spots' for oxidative damage. Few studies have measured the distance over which oxidative damage may travel through DNA. Here, we have prepared electron transfer assemblies in which an oxidizing intercalator is covalently tethered to one end of an oligonucleotide duplex containing a 5′-GG-3′ sequence. By employing a well-characterized flash–quench technique, we have demonstrated oxidation of 5′-GG-3′ sequences separated from the Ru(III) oxidant by ~11 bp (~37 Å). Hence, long-range charge migration is not only apparent with photooxidants but can also be demonstrated with a ground-state oxidant. Furthermore, long-range oxidation of DNA occurs in high yield using the flash–quench method and leads to formation of 8-oxo-G, a common cellular lesion.

By varying the base sequence in these assemblies, we may begin to characterize features of charge migration in DNA. Experiments in which the 5′-GG-3′ doublet is mutated to a 5′-GC-3′ sequence demonstrate that positive charge migrates through the helix on a timescale that is faster than the time required for trapping of the radical. Moreover, results point to the equilibration of charge to the sites of lowest energy. The mechanism underlying this charge migration, such as tunneling or hopping, still needs to be elucidated. The long-range chemistry is also sensitive to the presence of mismatches. Here, we have shown that G•A mispairs are more readily oxidized than G•T mispairs and that their presence affects the yield of oxidative damage of a 5′-GG-3′ doublet beyond the mismatch. Thus, this chemistry may be useful for the detection of mismatches in duplex DNA. Given the versatility and efficiency of this reaction, the flash–quench method described here provides a useful new probe of the DNA helix and its chemistry. Indeed, this chemical reactivity of DNA needs to be considered within the biological context of the cell.

Materials and methods

Materials

Oligonucleotides were prepared on an Applied Biosystems 394 DNA synthesizer, using standard phosphoramidite chemistry [66,67]. Duplexes were formed by slow cooling of equal concentrations of complementary strands. $Ru(phen)_2(dppz)^{2+}$ was prepared as described previously [68]. The quenchers $[Ru(NH_3)_6]Cl_3$, methyl viologen dichloride, and $[Co(NH_3)_5Cl]Cl_2$ were purchased from Aldrich and used as received. $Ru(phen)(bpy')(Me_2dppz)^{2+}$-modified oligonucleotides were prepared from the racemic metal complex. This trisheteroleptic complex was synthesized according to the general method of Strouse *et al.* [69] and Anderson *et al.* [64]; the two isomers of *rac*-$[Ru(phen)(bpy')(Me_2dppz)]^{2+}$ (with the carboxylate arm axial or equatorial to the Me_2dppz ligand) were not separated. Both metal complex isomers were conjugated to the oligonucleotide by a solid-phase methodology as follows. The oligonucleotide was prepared with an ABI 394 DNA synthesizer using standard solid-phase methodologies [66,67]. The linker $NH_2(CH_2)_9NHCO$- was added to resin-bound DNA at the 5′ sugar [70]. Coupling of metal complex to the amino-terminated DNA was then accomplished by stirring a slurry of $Ru(phen)(bpy')(Me_2dppz)Cl_2$ (7 μmol), hydroxyazobenzotriazole (14 μmol), N,N′-diisopropylethylamine (14 μmol), and resin-bound DNA (2 μmol) in 400 μl dimethylformamide [71–73]. After 12 h, the resin was rinsed and the Ru(II)–DNA conjugate cleaved and deprotected by treatment with 2 ml NH_4OH at 55°C for 6 h. Purification was achieved by HPLC (Hewlett Packard HP1050, Dynamax C4 or C18, 300 Å column (Rainin)). HPLC conditions were as follows: solvent A = NH_4OAc buffer (100 mM), pH 6.5; solvent B = CH_3CN; gradient = 5–25% B over 40 min to elute DNA and Ru(II)–DNA, 25–50% B over 10 min to elute unconjugated metal complex. Coupling of the two metal complex isomers to DNA led to formation of Δ- and Λ- diastereomeric conjugates; the reaction thus gave four products. The first Δ-isomer that elutes was used in all studies. Ru(II)–DNA conjugates were characterized by UV–visible spectroscopy ($\varepsilon_{440} = 1.9 \times 10^4\ M^{-1}\ s^{-1}$), circular dichroism spectroscopy, electrospray ionization mass spectrometry, and enzymatic digestion.

Assays of oxidative products

Strands were 5′^{32}P-end-labeled (*) by standard protocols [74] and hybridized to either the Ru(II)-modified or unmodified complementary strands in an aerated buffer of 5 mM phosphate, 50 mM NaCl, pH 7. Oligonucleotide duplexes (8 μM) containing 10–20 equivalents of quencher were irradiated at 436 nm with a 1000 W Hg/Xe lamp equipped with a monochromator (~6 mW at 442 nm); for the experiments on duplexes containing mismatches the power was ~70 mW at 442 nm. Irradiation with a CW He-Cd laser (~25 mW at 442 nm) yielded similar results. Irradiation times varied from 10 s to 60 min. After irradiation, samples were treated with 100 μl of 1 M piperidine at 90°C for 30 min, dried, and electrophoresed through a 20% denaturing polyacrylamide gel. The extent of damage was quantitated by phosphorimagery (Imagequant).

To characterize the products of oxidative damage, samples (200 μl) containing oligonucleotide (10 μM), Ru(II) complex (10 μM) and quencher (200 μM) were irradiated as described above. DNA was then digested (2 h each) with nuclease P_1 (Boehringer Mannheim) and then alkaline phosphatase (Boehringer Mannheim) [32,37]. The resultant nucleosides were separated by HPLC (Hewlett Packard HP1090, Microsorb MV C18, 100 Å column (Rainin)) and identified by coelution with authentic standards (Caymen Chemicals). HPLC conditions were as follows: oven temperature = 40°C; solvent A = citric acid, NH_4OAc buffer, pH 5; solvent B = CH_3OH; gradient = 1–4% B over 40 min.

Quantum yield determinations

Emission quantum yields were measured on an SLM8000 steady-state fluorimeter and were determined relative to $\Phi_{Ru(bpy)3^{2+}} = 0.012$ in aerated CH_3CN [75]. To determine the quantum yield of damage, samples (20 μl) were irradiated at 436 nm, treated with piperidine, and analyzed by gel electrophoresis (*vide supra*). The yield of damage was then quantitated by phosphorimagery and was not corrected for the <1.5% strand scission/G detected in control experiments with piperidine-treated DNA. Using the same geometry as for sample irradiations, ferrioxalate actinometry [76] was conducted to determine light intensity. The quantum yield of damage (Φ_{damage}) was then calculated as moles of strand breaks/moles photons. Care was taken to perform actinometry

and cleavage experiments under the same conditions, and several trials were run to ensure precision. Light intensity was calculated from

$$I = (A_{510})(V_{irr})(V_{final}) / (\varepsilon)(\Phi_{436})(t)(V_{Fe})$$

where I = light intensity in Einsteins/s; A_{510} = absorbance of actinometry solution of volume V_{final} (ml); V_{irr} = volume of irradiated sample (l); ε = extinction coefficient of $Fe(phen)_3^{2}$; Φ_{436} = quantum yield of actinometer; t = time (s); V_{Fe} = volume of ferrioxalate solution (ml).

Acknowledgements

We are grateful to the NIH (GM 49216) for their financial support of this work. In addition, we thank the NIH for predoctoral trainee support (M.R.A.) and a postdoctoral fellowship (S.C.P.), and the American Cancer Society for postdoctoral support (E.D.A.S.). We also thank J. Winkler for helpful discussions.

References

1. O'Neill, P. & Fielden, E.M. (1993). Primary free-radical processes in DNA. *Adv. Radiat. Biol.* **17**, 53–120.
2. Meade, T.J. (1996). Electron-transfer reactions through the DNA double helix. *Met. Ions Biol. Syst.* **32**, 453–478.
3. Stemp, E.D.A. & Barton, J.K. (1996). Electron-transfer between metal-complexes bound to DNA – is DNA a wire. *Met. Ions Biol. Syst.* **33**, 325–365.
4. Snart, R.S. (1968). Photoelectric effects of deoxyribonucleic acid. *Biopolymers* **6**, 293–297.
5. O'Konski, C.T., Moser, P. & Shirai, M. (1964). Electric properties of macromolecules .XI. Conductivity and dielectric constant of solid sodium, lithium and magnesium deoxyribonucleates. *Biopol. Symp.* **1**, 479–500.
6. Van Lith, D., de Haas, M.P., Warman, J.M. & Hummel, A. (1983). Highly mobile charge-carriers in hydrated DNA and collagen formed by pulsed ionization. *Biopolymers* **22**, 807–810.
7. Melvin, T., Plumb, M.A., Botchway, S.W., O'Neill, P. & Parker, A.W. (1995). 193 nm light induces single-strand breakage of DNA predominantly at guanine. *Photochem. Photobiol.* **61**, 584–591.
8. Melvin, T., Botchway, S.W., Parker, A.W. & O'Neill, P. (1995). Migration of photoinduced oxidative damage in models for DNA. *J. Chem. Soc. Chem. Comm.* **6**, 653–654.
9. Cullis, P.M., McClymont, J.D. & Malone, M.E. (1992). Effects of ionizing-radiation on deoxyribonucleic-acid. 7. Electron-capture at cytosine and thymine. *J. Chem. Soc. Perkins Trans. 2* **10**, 1695–1702.
10. Cullis, P.M., McClymont, J.D. & Symons, M.C.R. (1990). Electron conduction and trapping in DNA – an electron-spin-resonance study. *J. Chem. Soc. Faraday Trans.* **86**, 591–592.
11. Al-Kazwini, A.T., O'Neill, P., Adams, G.E. & Fielden, E.M. (1990). Radiation-induced energy migration within solid DNA – the role of misonidazole as an electron trap. *Radiat. Res.* **121**, 149–153.
12. Anderson, R.F., Patel, K.B. & Wilson, W.R. (1991). Pulse-radiolysis studies of electron migration in DNA from DNA base-radical anions to nitroacridine intercalators in aqueous-solution. *J. Chem. Soc. Faraday Trans. 1.* **87**, 3739–3746.
13. Pezeshk, A., Symons, M.C.R. & McClymont, J.D. (1996). Electron movement along DNA strands – use of intercalators and electron-paramagnetic-resonance spectroscopy. *J. Phys. Chem.* **100**, 18562–18566.
14. Arkin, M.R., *et al.*, & Barbara, P.F. (1996). Rates of DNA-mediated electron transfer between metallointercalators. *Science* **273**, 475–480.
15. Baguley, B.C. & LeBret, M. (1984). Quenching of DNA-ethidium fluorescence by amsacrine and other antitumor agents: a possible electron-transfer effect. *Biochemistry* **23**, 937–943.
16. Baguley, B.C. (1990). The possible role of electron-transfer complexes in the antitumor action of amsacrine analogues. *Biophys. Chem.* **35**, 203–212.
17. Brun, A.M. & Harriman, A. (1992). Dynamics of electron transfer between intercalated polycyclic molecules: effect of interspersed bases. *J. Am. Chem. Soc.* **114**, 3656–3660.
18. Brun, A.M. & Harriman, A. (1994). Energy-transfer and electron-transfer processes involving palladium. *J. Am. Chem. Soc.* **116**, 10383–10393.
19. Holmlin, R.E., Stemp, E.D.A. & Barton, J.K. (1996). $Os(phen)_2dppz^{2+}$ in photoinduced DNA-mediated electron-transfer reactions. *J. Am. Chem. Soc.* **118**, 5236–5244.
20. Houee-Levin, C., Gardes-Albert, M., Rouscilles, A., Ferradini, C. & Hickel, B. (1991). Intramolecular semiquinone disproportionation in DNA - pulse-radiolysis study of the one-electron reduction of daunorubicin intercalated in DNA. *Biochemistry* **30**, 8216–8222.
21. Meade, T.J. & Kayyem, J.F. (1995). Electron transfer through DNA: site-specific modification of duplex DNA with ruthenium donors and acceptors. *Angew. Chem. Int. Ed. Engl.* **34**, 352–354.
22. Murphy, C.J., *et al.*, & Barton, J.K. (1993). Long-range photoinduced electron-transfer through a DNA helix. *Science* **262**, 1025–1029.
23. Murphy, C.J., Arkin, M.R., Ghatlia, N.D., Bossmann, S., Turro, N.J. & Barton, J.K. (1994). Fast photoinduced electron-transfer through DNA intercalation. *Proc. Natl. Acad. Sci.* **91**, 5315–5319.
24. Stemp, E.D.A., Arkin, M.R. & Barton, J.K. (1995). Electron transfer between metallointercalators bound to DNA: spectral identification of the transient intermediate. *J. Am. Chem. Soc.* **117**, 2375–2376.
25. Fromherz, P. & Rieger, B. (1986). Photoinduced electron-transfer in DNA matrix from intercalated ethidium to condensed methylviologen. *J. Am. Chem. Soc.* **108**, 5361–5362.
26. Otto, P., Clementi, E. & Ladik, J. (1983). The electronic-structure of DNA related periodic polymers. *J. Chem. Phys.* **78**, 4547–4551.
27. Priyadarshy, S., Risser, S.M. & Beratan, D.N. (1996). DNA is not a molecular wire: protein-like electron-transfer predicted for an extended π-electron system. *J. Phys. Chem.* **100**, 17678–17682.
28. Risser, S.M., Beratan, D.N. & Meade, T.J. (1993). Electron-transfer in DNA – predictions of exponential-growth and decay of coupling with donor-acceptor distance. *J. Am. Chem. Soc.* **115**, 2508–2510.
29. Sugiyama, H. & Saito, I. (1996). Theorical-studies of GC-specific photocleavage of DNA via electron-transfer: significant lowering of ionization-potential and 5′-localization of HOMO of stacked GG bases in B-form DNA. *J. Am. Chem. Soc.* **118**, 7063–7068.
30. Dee, D. & Baur, M.E. (1974). Charge and excitation migration in DNA chains. *J. Chem. Phys.* **60**, 541–560.
31. Felts, A.K., Pollard, W.T. & Friesner, R.A. (1995). Multilevel redfield treatment of bridge-mediated long-range electron-transfer – a mechanism for anomalous distance dependence. *J. Phys. Chem.* **99**, 2929–2940.
32. Hall, D.B., Holmlin, R.E. & Barton, J.K. (1996). Oxidative DNA-damage through long-range electron-transfer. *Nature* **382**, 731–735.
33. Hall, D.B. & Barton, J.K. (1997). Sensitivity of DNA-mediated electron transfer to the intervening π-stack: a probe for the integrity of the DNA base stack. *J. Am. Chem. Soc.*, in press.
34. Ly, D., Kan, Y., Armitage, B. & Schuster, G.B. (1996). Cleavage of DNA by irradiation of substituted anthraquinones – intercalation promotes electron-transfer and efficient reaction at GG steps. *J. Am. Chem. Soc.* **118**, 8747–8748.
35. Armitage, B., Yu, C., Devadoss, C. & Schuster, G.B. (1994). Cationic antraquinone derivatives as catalytic DNA photonucleases – mechanisms for DNA-damage and quinone recycling. *J. Am. Chem. Soc.* **116**, 9847–9859.
36. Dunn, D.A., Lin, V.H. & Kochevar, I.E. (1992). Base-selective oxidation and cleavage of DNA by photochemical cosensitized electron-transfer. *Biochemistry* **31**, 11620–11625.
37. Ito, K., Inoue, S., Yamamoto, K. & Kawanishi, S. (1993). 8-hydroxydeoxyguanosine formation at the 5′ site of 5′-GG-3′ sequences in double-stranded DNA by UV-radiation with riboflavin. *J. Biol. Chem.* **268**, 13221–13227.
38. Saito, I., Takayama, M., Sugiyama, H., Nakatani, K., Tsuchida, A. & Yamamoto, M. (1995). Photoinduced DNA cleavage via electron-transfer: demonstration that guanine residues located 5′ to guanine are the most electron-donating sites. *J. Am. Chem. Soc.* **117**, 6406–6407.
39. Johnston, D.H., Glasgow, K.C. & Thorp, H.H. (1995). Electrochemical measurement of the solvent accessibility of nucleobases using electron-transfer between DNA and metal-complexes. *J. Am. Chem. Soc.* **117**, 8933–8938.
40. Manoharan, M., Tivel, M.L., Zhao, M., Nafisi, K. & Netzel, T.L. (1995). Base-sequence dependence of emission lifetimes for DNA oligomers and duplexes covalently labeled with pyrene – relative electron-transfer quenching efficiences of A-nucleoside, G-nucleoside, and T-nucleoside toward pyrene. *J. Phys. Chem.* **99**, 17461–17472.
41. Breslin, D. & Schuster, G.D. (1996). Anthraquinone photonucleases – mechanisms for GG-selective and nonselective cleavage of double-stranded DNA. *J. Am. Chem. Soc.* **118**, 2311–2319.
42. Dandliker, P.J., Holmlin, R.E. & Barton, J.K. (1997). Oxidative thymine dimer repair in the DNA helix. *Science* **275**, 1465–1468.
43. Stemp, E.D.A., Arkin, M.R. & Barton, J.K. (1997). Oxidation of guanine in DNA by $Ru(phen)_2dppz^{3+}$ using the flash-quench technique. *J. Am. Chem. Soc.* **119**, 2921–2925.

44. Friedman, A.E., Chambron, J.C., Sauvage, J.P., Turro, N.J. & Barton, J.K. (1990). Molecular light switch for DNA – $Ru(bpy)_2(dppz)^{2+}$. *J. Am. Chem. Soc.* **112**, 4960–4962.
45. Jenkins, Y., Friedman, A.E., Turro, N.J. & Barton, J.K. (1992). Characterization of dipyridophenazine complexes of ruthenium(II) – the light switch effect as a function of nucleic-acid sequence and conformation. *Biochemistry* **31**, 10809–10816.
46. Dupureur, C.M. & Barton, J.K. (1994). Use of selective deuteration and ^{1}H-NMR in demonstrating major groove binding of Δ-$[Ru(phen)_2dppz]^{2+}$ to $d(GTCGAC)_2$. *J. Am. Chem. Soc.* **116**, 10286–10287.
47. Dupureur, C.M. & Barton, J.K. (1997). Structural studies of Λ-$[Ru(phen)_2dppz]^{2+}$ and Δ-[Ru(phen)2dppz]2+ Bound to $d(GTCGAC)_2$ – characterization of enantioselective intercalation. *Inorg. Chem.* **36**, 33–43.
48. Chang, I.J., Gray, H.B. & Winkler, J.R. (1991). High-driving-force electron-transfer in metalloproteins - intramolecular oxidation of ferrocytochrome-c by $Ru(2,2'\text{-bpy})_2(Im)(His\text{-}33)^{3+}$. *J. Am. Chem. Soc.* **113**, 7056–7057.
49. Murphy, C.J. & Barton, J.K. (1993). Ruthenium complexes as luminescent reporters of DNA. *Methods Enzymol.* **226**, 576–594.
50. Mei, H.Y. & Barton, J.K. (1988). Tris(tetramethylphenanthroline)ruthenium(II): a chiral probe that cleaves A-DNA conformations. *Proc. Natl. Acad. Sci.* **85**, 1339–1343.
51. Mei, H.Y. & Barton, J.K. (1986). Chiral probe for A-form helices of DNA and RNA – tris(tetramethylphenanthroline)ruthenium(II). *J. Am. Chem. Soc.* **108**, 7414–7416.
52. Chung, M.-H., Kiyosawa, H., Nishimura, S. & Kasai, H. (1992). DNA strand cleavage at 8-hyroxyguanine residues by hot piperidine treatment. *Biochem. Biophys. Res. Comm.* **188**, 1–7.
53. Rougee, M. & Bensasson, R.V. (1986). Determination of the decay-rate constant of singlet oxygen $^1\Delta_g$ in presence of biomolecules. *Cr. Acad. Sci. Ser. 2.* **302**, 1223–1226.
54. Arkin, M.R., Stemp, E.D.A., Turro, C., Turro, N.J. & Barton, J.K. (1996). Luminescence quenching in supramolecular systems - a comparison of DNA-mediated and SDS Micelle-mediated photoinduced electron-transfer between metal-complexes. *J. Am. Chem. Soc.* **118**, 2267–2274.
55. Rodgers, M.A.J. & Snowden, P.T. (1982). Lifetime of O_2 ($^1\Delta_g$) in liquid water as determined by time-resolved infrared luminescence measurements. *J. Am. Chem. Soc.* **104**, 5541–5543.
56. Atherton, S.J. & Beaumont, P.C. (1987). Laser flash-photolysis of DNA-intercalated ethidium-bromide in the presence of methylviologen. *J. Phys. Chem.* **91**, 3993–3997.
57. Cullis, P.M., Malone, M.E. & Merson-Davies, L.A. (1996). Guanine radical cations are precursors of 7,8-dihydro-8-oxo-2′-deoxyguanosine but are not precursors of immediate strand breaks in DNA. *J. Am. Chem. Soc.* **118**, 2775–2781.
58. Barciszewski, J., Barciszewska, M.Z., Rattan, S.I.S. & Clark, B.F.C. (1995). The structure and properties of 8-hydroxy-2′-deoxyguanosine – a novel biomarker in aging and carcinogenesis studies. *Polish J. Chem.* **69**, 841–851.
59. Shibutani, S., Takeshita, M. & Grollman, A.T. (1991). Insertion of specific bases during DNA-synthesis past the oxidation-damaged base 8-oxoG. *Nature* **349**, 431–434.
60. Hunter, W.N., Brown, T., Anand, N.N. & Kennard, O. (1986). Structure of an adenine cytosine base pair in DNA and Its implications for mismatch repair. *Nature* **320**, 552–555.
61. Hunter, W.N., Brown, T., Kneale, G., Anand, N.N., Rabinovich, D. & Kennard, O. (1987). The structure of guanosine-thymidine mismatches in B-DNA at 2.5 Å resolution. *J. Biol. Chem.* **262**, 9962–9970.
62. Kennard, O. (1985). Structural studies of DNA fragments: The G T wobble base pair in A, B, and Z DNA; The G A base pair in B-DNA. *J. Biomol. Struct. Dyn.* **3**, 205–226.
63. Sitlani, A., Long, E.C., Pyle, A.M. & Barton, J.K. (1992). DNA photocleavage by phenanthrenequinone diimine complexes of rhodium(III): shape-selective recognition and reaction. *J. Am. Chem. Soc.* **114**, 2303–2312.
64. Anderson, P.A., *et al.*, & White, A.H. (1995). Designed synthesis of mononuclear tris(heteroleptic) ruthenium complexes containing bidentate polypyridyl ligands. *Inorg. Chem.* **34**, 6145–6157.
65. Turro, C., Evenzahav, A., Bossmann, S.H., Barton, J.K. & Turro, N.J. (1996). Excited-state properties of $Rh(phi)_2phen^{3+}$ and related complexes: strong photooxidant. *Inorg. Chim. Acta.* **243**, 101–108.
66. Beaucage, S.L. & Caruthers, M.H. (1981). Deoxynucleoside phosphoramidites – a new class of key intermediates for deoxypolynucleotide synthesis. *Tetrahedron Letters.* **22**, 1859–1802.
67. Goodchild, J. (1990). Conjugates of oligonucleotides and modified oligonucleotides: a review of their synthesis and properties. *Bioconjugate Chemistry* **1**, 165–187.
68. Amouyal, E., Homsi, A., Chambron, J.-C. & Sauvage, J.-P. (1990). Synthesis and study of a mixed-ligand ruthenium(II) complex in its ground and excited states: Bis(2,2′-bipyridine)(dipyrido[3,2-*a*:2′,3′-c]phenazine-(N^4N^5)ruthenium(II). *J. Chem. Soc. Dalton Trans.*, 1841–1845.
69. Strouse, G.F., Anderson, P.A., Schoonover, J.R., Meyer, T.J. & Keene, F.R. (1992). Synthesis of polypyridyl complexes of ruthenium(II) containing 3 different bidentate ligands. *Inorg. Chem.* **31**, 3004–3006.
70. Wachter, L., Jablonski, J.-A. & Ramachandran, K.L. (1986). A simple and efficient procedure for the synthesis of 5′-aminoalkyl oligonucleotides. *Nucleic. Acids Res.* **14**, 7985–7994.
71. Angell, Y.M., Garcia-Echeverria, C. & Rich, D.H. (1994). Comparative-studies of the coupling of N-methylated, sterically hindered amino-acids during solid-phase peptide-synthesis. *Tetrahedron Letters* **35**, 5981–5984.
72. Carpino, L.A. & El-Faham, A. (1994). Effect of tertiary bases on O-benzotriazolyluronium salt-induced peptide segment coupling. *J. Org. Chem.* **59**, 695–698.
73. Carpino, L.A., El-Faham, A. & Albericio, F. (1994). Racemization studies during solid-phase peptide-synthesis using azabenzotriazole-based coupling reagents. *Tetrahedron Letters* **35**, 2279–2282.
74. Sambrook, J., Fritsch, E.F. & Maniatis, T. (1989). *Molecular Cloning: a Laboratory Manual.* (2nd), Cold Spring Harbor Laboratory Press, New York, NY, USA.
75. Calvert, J.M., Caspar, J.V., Binstead, R.A., Westmoreland, T.D. & Meyer, T.J. (1982). Metallopolymer photochemistry. Photophysical, photochemical, and photo-electrochemical properties of $(bpy)_2Rull<$ sites bound to poly(4-vinylpyridine). *J. Am. Chem. Soc.* **104**, 6620–6627.
76. Calvert, J. G. & Pitts, J. N. J. (1966). *Photochemistry.* John Wiley and Sons, Inc., New York, USA.